

Thermo reflectance bolometry

S. V. Mitko,^{a)} A. Yu. Oudalov, Yu. B. Udalov, P. J. M. Peters, and K. J. Boller
*Laser Physics and Non-linear Optics Group, Faculty of Natural Sciences, University of Twente,
 P.O. Box 217, 7500 AE, Enschede, The Netherlands*

(Received 20 September 2004; accepted 4 October 2004; published online 17 December 2004)

An approach to bolometry has been developed. It is based on the measurements of optical reflectivity change of a thin metal layer deposited on a transparent substrate. The reflectivity change results from the temperature rise due to absorption of energetic particles or x rays. The sensor of the bolometer has no ohmic contact with the measuring unit, making this method well suited for an environment with strong electromagnetic noise interference. The technique was applied to characterize a method for the generation of intense electron beams in a dense gas. Very high efficiency for the e-beam generation (up to 95%) was measured. © 2005 American Institute of Physics. [DOI: 10.1063/1.1823655]

I. INTRODUCTION

There exist three groups of bolometers, which differ by the temperature transducer types. The best known and most widely used are the so-called “resistive” bolometers originally developed by Langley¹ in 1881, and the “pyroelectric” bolometers. These, correspondingly, make use of a temperature driven change in the electric resistivity or in the dielectric constant of the sensor material.² The infrared bolometry utilizes the infrared radiation of the sensing element to measure its temperature.³

All these techniques have some drawbacks. The resistive and pyroelectric bolometries rely on contact measurements of the electric resistance or the dielectric constant, thus requiring two electric circuits: one to drive the bolometer and another one for readout. The presence of two cables acting as a ground/pickup loop results in additional electromagnetic interference.⁴ Moreover, the measurements of intense fluxes of charged particles are complicated with these techniques, as an electric current associated with the particle flux would result in false readings. The infrared bolometry suffers from its poor sensitivity, as it is necessary to measure the radiation flux produced by a minor (in the order of 10 °C) temperature change of the sensor with a small area (<1 cm²) located at substantial distance (>50 cm) from an infrared detector.

A thermo reflectance bolometry proposed by us does not have these drawbacks. In the suggested approach a change in the optical reflectance coefficient of a sensor element resulting from its temperature change is measured. Thus, it combines the attractive features of resistive bolometry such as high sensitivity with noncontact sensing specific of infrared bolometry. The sensitivity increase is achieved due to higher intensity of the incident light. The effect is somewhat similar to the impact of higher magnitude of a reference current or a voltage in resistive bolometry.

The physical property of materials to change their reflectance with temperature is well known⁵ and has a wide range

of applications such as studies of the band structures of semiconductors⁶ or the measurements of thermo physical constants of thin surface films.⁷ The only application of this property in the gas discharge physics was done for the estimation of electrode temperature evolution during starting up of high-pressure arc lamps.⁸ However, as far as we know it has never been used for bolometry.

The main purpose of the present work is to develop a bolometer capable of measurements of electron beam and soft x ray energy directly in a gas environment. Powerful electron beams are generated in an open barrier discharge electron gun⁹ and other devices based on an open discharge principle,^{10,11} but the efficiency of these devices is still unknown, mainly due to the absence of an appropriate measurement technique.

II. BOLOMETER ELEMENT SELECTION AND FABRICATION

A proper bolometer design assumes a compromise between its sensitivity on the one hand and its opacity for the radiation to be measured on the other. For several reasons we have chosen thin chromium films as sensor material for our bolometers. The thermo reflectance spectrum of chromium has a wide peak at the wavelength of $\sim 1 \mu\text{m}$.¹² This wavelength region ideally coincides with a maximal response of most Si photodiodes. Also, an incandescent halogen lamp is a convenient illumination source in this spectral range. Chromium is sufficiently a dense material, thus the electrons with the energy of $\sim 20 \text{ keV}$ can be stopped in the films of sub-micron thicknesses. Meanwhile, the backscattering energy coefficient of chromium does not exceed ~ 0.2 thus the corrections due to electron backscattering are small compared to heavier materials like Ni, Cu, Au, etc. The technology of chromium coating deposition is very well developed as it is often used as an adhesion layer for other metal coatings. Thus if one wants to increase the opacity of the bolometer in order to measure the radiation of higher energy, it can be easily done by depositing an extra layer of the material that is denser than chromium on top of the original layer.

^{a)} Author to whom correspondence should be addressed; electronic mail: s.v.mitko@ewi.utwente.nl

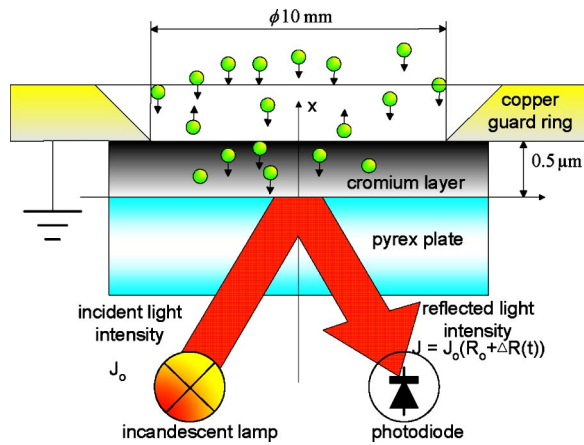


FIG. 1. (Color online) Sketch of thermo reflectance bolometer.

In our design a sensing element of the bolometer consists of a thin (up to $1\ \mu\text{m}$) chromium film, which is 3 cm wide and 3 cm long. To ensure a rugged design, the film is deposited onto a thick transparent substrate with low thermal conductivity such as Pyrex or Quartz. An electron beam evaporator (model Balzers BAK 600) is used in the deposition process. Fairly reproducible properties of the evaporated films as concerned with the thermo reflectance coefficient and the mass thickness were obtained with the residual gas pressure of 10^{-7} mbar and the deposition speed of $5\ \text{A s}^{-1}$. The specific electric resistivity of the film was measured to be about ten times the bulk material resistivity.

The opacity of the bolometer for the incident electron beam or x rays is determined by its mass thickness. The mass thickness of the evaporated films was measured by direct weighing of the substrate plate before and after the evaporation. Sartorius ME215P balance with an accuracy of 2% was used for these measurements. The measurements of the film thickness with the surface profilometer (model Veeco Dektak 8) confirmed that the mass density of the evaporated film is equal to the mass density of the bulk material with an accuracy better than 5% for the film thicknesses between 0.5 and $1\ \mu\text{m}$.

A schematic diagram of thermo reflectance bolometer is sketched in Fig. 1. X rays or energetic electrons reach the metal film through an opening in a protecting ring. This ring serves both as a holder for the sensor and as its ground connector. The energetic particles or radiation are absorbed in the bolometer film. As their energy is transferred into heat the film temperature rises. The rate of this process is determined by the specific heat of the material and the heat diffusion into the substrate. The metal/substrate interface is illuminated with an external light source. The temperature change alters optical reflectance at the interface thus modulating the intensity of the reflected light. An appropriate fast photodetector measures the intensity of reflected light. The interface temperature as well as the incident power and/or energy are determined in this way.

III. BOLOMETER RESPONSE TO X RAYS AND ELECTRON BEAMS

The high spectrally flat opacity for the incident radiation is the real concern for reliable measurements of incoming

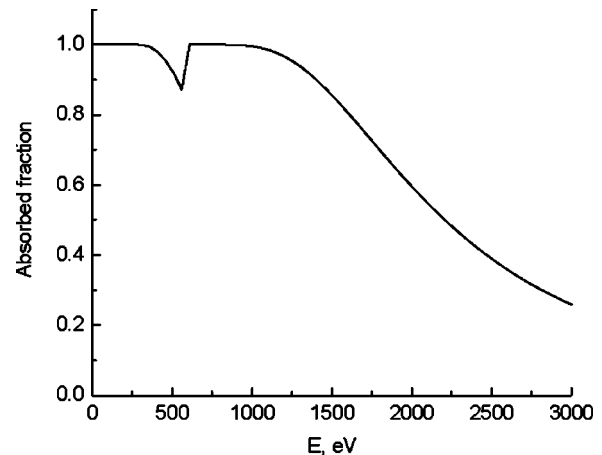
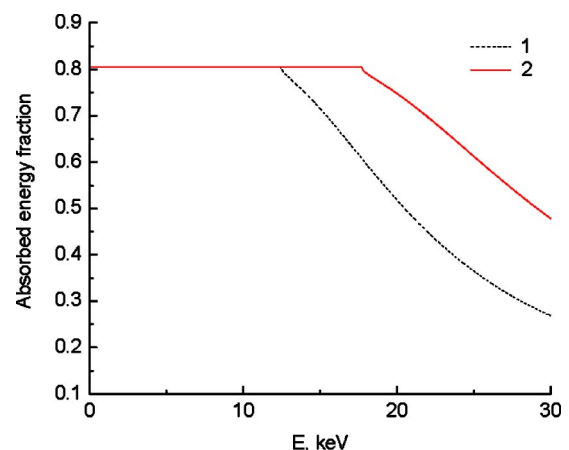


FIG. 2. Absorbed fraction of x rays as a function of photon energy.

energy flux with any bolometer. The fractional absorption of x rays in a $1\text{-}\mu\text{m}$ -thick chromium film is shown in Fig. 2. The data tabulated in Ref. 13 were used in these calculations. It is seen that the spectral response of the element is nearly flat up to $1.2\ \text{keV}$. In this sense our bolometer design could be seen as an alternative to resistive bolometers extensively used to measure x rays generated by high power Z pinches and Z accelerators.⁵ The main advantage, however, will be a substantial reduction of electromagnetic interference.

In order to determine the opacity of the bolometer for x rays it is sufficient to know the mass absorption coefficient. To the contrary, the estimation of the bolometer opacity in the case of electrons is more complex. The energy of an incident electron beam dissipates in several ways. Part of the electrons is reflected from the target in a backscattering process, so their energy will not be measured. Another part of initial beam energy is transferred by electrons that pass through the metal film. This part is proportional to the transmittance coefficient multiplied by the average energy of transmitted electrons. The rest of the incident beam energy is absorbed in the metal film thus defining its opacity. The absorbed fraction of the electron beam energy for chromium films with thicknesses of 0.5 and $1\ \mu\text{m}$ is shown in Fig. 3. The experimental data^{14–16} for copper were recalculated for

FIG. 3. (Color online) Absorbed energy fraction as a function of electron energy. 1-chromium film, thickness $0.5\ \mu\text{m}$; 2-chromium film, thickness $1\ \mu\text{m}$.

chromium thin films using semiempirical equations.^{17–19} Here a small energy fraction reflected from the supporting glass substrate back into the metal film was neglected as it constitutes $\sim 5\%$ of the total transmitted energy.⁷

It is seen in Fig. 3 that the response of the bolometer is flat in the range of low electron energies defined by the thickness of the metal film. As the energy increases further the electrons start to penetrate the film and the fraction of absorbed energy drops abruptly. The maximum fraction of the energy absorbed in the film is less than unity due to the backscattered electrons.

The power absorption in the metal film results in the rise of the temperature at metal/substrate interface. There exists an analytical relationship between the temperature change and the absorbed power. This relation holds true even in the case when the cooling of the metal film due to heat absorption in the substrate plays a dominant role in the overall energy balance. The absorbed power $P(t)$ depends on the change of the metal/substrate interface temperature as follows (see the Appendix for details):

$$P(t) = c_m \rho_m h \frac{d}{dt} T(t) + \sqrt{\frac{\lambda_g c_g \rho_g}{\pi}} \int_0^t d\xi \frac{d}{d\xi} T(\xi) \frac{1}{\sqrt{t-\xi}} \quad (1)$$

Here c_m , ρ_m , c_g , ρ_g are the specific heat capacity and the density of the metal film and of the substrate, respectively, h is the thickness of the film and λ_g is the thermal conductivity of the substrate. One can clearly see that it is preferable to use substrates with a small λ_g . In the opposite case power loss due to the heat diffusion into the substrate, expressed by the second term on the right side of Eq. (1), should be taken into account. Thus, it is sufficient to know the interface temperature alone in order to determine the absorbed power.

The relationship between the temperature change and the observed photodiode response is defined by the following equation:

$$\frac{d}{dt} U(t) + U(t) = \xi T(t). \quad (2)$$

Here $U(t)$ is the photodiode response, $\xi = dR/RdT$ is the thermo reflectance coefficient, where R in turn is the reflectivity of the interface and τ is the response time of the photodiode. The photodiode response is as follows:

$$U(t) = \frac{V(t) - V_0}{V_0}. \quad (3)$$

Here $V(t)$ is the time dependent photodiode signal and V_0 is the reference signal.

A proper choice of the photodiode is of great importance for reliable operation of the thermo reflectance bolometer. The photodiode should have high quantum efficiency in the vicinity of $0.8 \mu\text{m}$, the wavelength corresponding to the maximum thermo reflectance response of the chromium thin film. As the thermo reflectance coefficient ξ is very small ($\sim 4 \times 10^{-5}$), a large level of the reference signal V_0 is mandatory in order to get a measurable quantity of the difference $V(t) - V_0$. Photodiode response should be linear, even at high reference currents. Further, the photodiode output should not exhibit “long tails” associated with deep traps in a semicon-

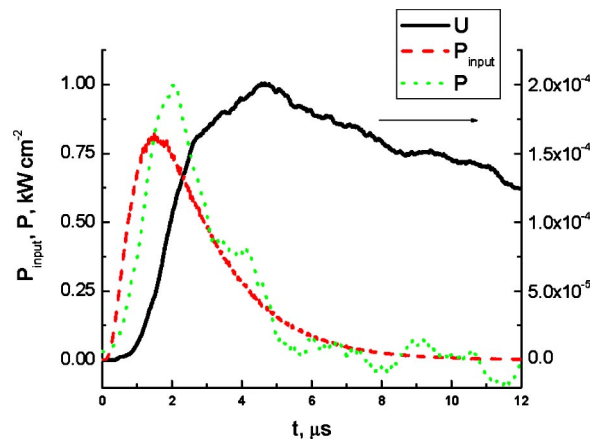


FIG. 4. (Color online) Pulses of the thermo reflectance signal U , input power P_{input} and calculated power P .

ductor material. A complete survey of the photodiodes available on the market has lead us to choose an EG&G FND100Q Si photodiode. It features a large saturation current (>10 mA), an absence of the delayed secondary response at times longer than 10 ns and a large aperture area of 2 mm in diameter. According to recommendations²⁰ the photodiode was biased at -50 V.

IV. CALIBRATION PROCEDURE AND THE PROOF OF PRINCIPLE EXPERIMENTS

In order to make an absolute calibration of the device the electrical pulse of known power and energy was absorbed by the bolometer and the resulting thermo reflectance signal was measured.²¹ This was done simply by discharging a capacitor charged up to a known potential through the bolometer film. Voltage drop as well as electric current were measured and the input power was calculated as their product. This way all the constants in Eqs. (1) and (2) could be determined. The result of this calibration procedure is shown in Fig. 4. Input power pulses $P_{\text{input}}(t)$ produced by the capacitor discharge, photodiode thermo reflectance signal $U(t)$ and power $P(t)$ derived with the use of Eqs. (1) and (2) are presented. The bolometer with a $0.5\text{-}\mu\text{m}$ -thick chromium film on Pyrex substrate was used. The response time of the photodiode circuit used in this experiment was ~ 400 ns. One can clearly see that besides energy measurements this straightforward and robust technique allows for power measurements provided the photodiode circuitry has an adequate linearity and temporal resolution.

The thermo reflectance bolometer was used to get quantitative data on the performance of a recently proposed electron beam generator, working in a dense gas. The electron beams with the current density of ~ 60 A/cm² and the electron energy of $\sim 10\text{--}20$ keV were produced by an open dielectric barrier discharge generator directly in a working gas at pressure up to ~ 100 mbar.⁹ The main problem in the evaluation of the energetic efficiency of the generator arises from the necessity to separate the power inputs from the electron beam itself and from the beam generating discharge. The detailed description of the working principle of the electron beam generator and experimental conditions is given in

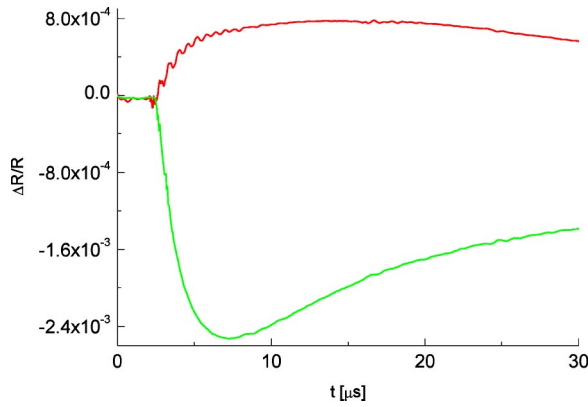


FIG. 5. (Color online) Bolometer response under the impact of the electron beam.

Ref. 9. For the sake of completeness we reproduce here some essential features. The electron beam is generated when a barrier discharge between two electrodes occurs. One of the electrodes is made of a metal mesh while the other is covered by a high ϵ dielectric. When the dielectric surface is charged negatively it acts as a cathode. The electrons are accelerated in a thin layer of cathode fall region and then expelled into the surrounding gas through the grid anode thus forming the electron beam. The peak beam current density as high as 60 A cm^{-2} was measured by the Faraday cup placed 3 cm apart from the grid anode at the charging voltage 20 kV. The discharge was produced in He gas at a pressure of 10 mbar in this experiment. To evaluate the energy efficacy of the electron beam production the Faraday cup was replaced by the bolometer while keeping other conditions similar. Typical traces of the bolometer response taken at the charging voltage of 17 kV are shown in Fig. 5. The upper trace corresponds to the bolometer made of chromium thin film with a thickness of $1 \mu\text{m}$ and the lower trace is measured with gold film bolometer with the thickness of less than $0.1 \mu\text{m}$. The negative sign of the latter is due to negative thermo reflectance coefficient of gold in spectral range used for illumination.²² This example shows that the observed signals are indeed of thermal nature and are not the result of illumination from the electron beam excited plasma or the pressure shock wave produced by the discharge. The dependence of the energy efficiency of the electron beam production on the charging voltage extracted from the similar data is shown in Fig. 6. The extremely high efficiency of the dielectric barrier discharge based generator is clearly seen.

While other known techniques failed in these harsh experimental conditions the thermo reflectance bolometer demonstrated excellent performance, high robustness and durability.

To summarize, the advantages of thermoreflectance bolometry are as follows: This is a broadband robust technique that measures absolute fluxes of energetic particles and/or electromagnetic radiation ranging from microwaves to soft x rays.

Noncontact remote sensing eliminates the problems of electromagnetic interference. The method is fast (response time up to $\sim 10 \text{ ns}$ could be easily achieved).

The signal to noise ratio is determined by the photodiode

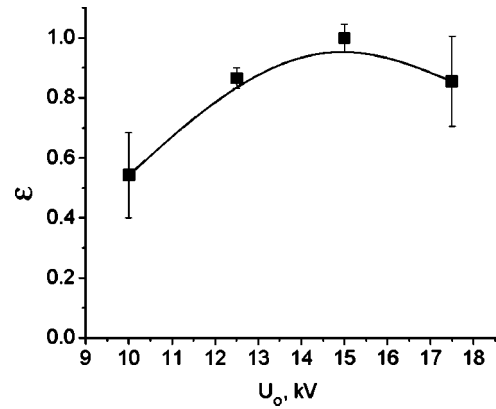


FIG. 6. Energy efficiency of the e-beam generator. Working gas He, pressure 10 mbar.

shot noise. This ratio can be further improved by using a high-power illuminating source. An incandescent lamp is ideally suited for this purpose.

ACKNOWLEDGMENTS

The kind assistance of A. Azarov in the preparation of experiments is highly acknowledged. The authors greatly appreciate the support of the Dutch Scientific Foundation (NWO) and the Stichting Technische Wetenschappen (STW) for enabling the stay of S.V.M at the University of Twente.

APPENDIX

The temperature fields in a metal layer and a glass substrate are described by the set of equations

$$c_m \rho_m \frac{\partial T_m(x,t)}{\partial t} = \lambda_m \frac{\partial^2 T_m(x,t)}{\partial x^2} + Q(x,t), \quad 0 < x < h, \quad (\text{A1})$$

$$c_g \rho_g \frac{\partial T_g(x,t)}{\partial t} = \lambda_g \frac{\partial^2 T_g(x,t)}{\partial x^2}, \quad -\infty < x < 0. \quad (\text{A2})$$

The boundary conditions are as follows:

$$\begin{aligned} \lambda_m \frac{\partial T_m(h,t)}{\partial x} &= W_s(h,t), \quad \lambda_m \frac{\partial T_m(0,t)}{\partial x} \\ &= \lambda_g \frac{\partial T_g(0,t)}{\partial x}, \quad T_m(0,t) = T_g(0,t). \end{aligned} \quad (\text{A3})$$

Here the x axis is perpendicular to the surface of metal and $c_m, \rho_m, \lambda_m, c_g, \rho_g, \lambda_g$ are the specific heat capacity, the mass density and the thermal conductivity of the metal and the glass, respectively. Two possible heat sources have been taken into account. The first one, $Q(x,t)$, is due to the energy lost inside the metal layer of thickness h by energetic particles or x rays. The second source $W_s(h,t)$ is due to the possible energy exchange between the metal layer and the surrounding environment.

The correctness the one-dimensional analysis (A1)–(A3) of the heat transfer process is justified by the fact that the distance L a thermal wave has to pass during typical electron beam generation process time is much smaller than the diameter of the bolometer. One can estimate L at $t=10 \mu\text{s}$ typical for our experimental conditions (see Fig. 4). Taking

$$L = (\lambda_m \tau / c_m \rho_m)^{1/2} \quad (\text{A4})$$

and substituting the data for chromium $c_m=0.452 \text{ Jg}^{-1} \text{ K}^{-1}$, $\lambda_m=0.94 \text{ W cm}^{-1} \text{ K}^{-1}$, $\rho_m=7.2 \text{ g cm}^{-3}$ into Eq. (A4) one gets $L \sim 17 \text{ } \mu\text{m}$. This length is much smaller than the diameter of the bolometer sensor (see Fig. 1.). This justifies our approximation.

Further analysis can be simplified by taking into account high value of thermal conductivity in metals λ_m as well as a small thickness of the metal film. Typical time $\tau = c_m \rho_m h^2 / \lambda_m \sim 8 \text{ ns}$ is needed for the temperature wave to pass through the metal. Thus the temperature difference across the metal film can be considered as a negligibly small for the time intervals longer than $\sim 10 \text{ ns}$. The two basic equations (A1) and (A2) can be effectively reduced to one equation now. This is done by integrating the first Eq. (A1) over x from 0 to h . Consequently, the temperature distribution over the metal film is averaged. Further, we assume that it is equal to the interface temperature. We introduce total power flux according to the following formula:

$$P(t) = W_s(t) + \int_0^h (x, t) dx. \quad (\text{A5})$$

As a result a complex problem (A1)–(A3) is reduced to a simplified one

$$c_g \rho_g \frac{\partial T_g(x, t)}{\partial t} = \lambda_g \frac{\partial^2 T_g(x, t)}{\partial x^2}, \quad -\infty < x < 0. \quad (\text{A6})$$

The respective boundary condition is now as follows:

$$c_m \rho_m \frac{\partial T_g(0, t)}{\partial t} = -\lambda_g \frac{\partial^2 T_g(0, t)}{\partial x^2} + P(t). \quad (\text{A7})$$

This problem is solved in a closed form by the method of Laplace transform.²³ It leads to Eq. (1).

¹ S. P. Langley, *Science* **2**, 11 (1881).

² P. L. Richards, *J. Appl. Phys.* **76**, 1 (1994).

³ J. C. Ingraham and G. M. Miller, *Rev. Sci. Instrum.* **54**, 673 (1983).

⁴ R. B. Spielman *et al.*, *Rev. Sci. Instrum.* **70**, 651 (1999).

⁵ *Optical Properties of Solids*, edited by F. Abeles (North-Holland, Amsterdam, 1972), pp. 253–257.

⁶ E. Matatagui, A. G. Thompson, and M. Cardona, *Phys. Rev.* **176**, 950 (1968).

⁷ D. Chu *et al.*, *J. Vac. Sci. Technol. B* **19**, 2874 (2001).

⁸ H. Kempkens, W. W. Byszewski, P. D. Gregor, and W. P. Lapatovich, *J. Appl. Phys.* **67**, 3618 (1989).

⁹ S. V. Mitko *et al.*, *Appl. Phys. Lett.* **83**, 2760 (2003).

¹⁰ P. A. Bokhan, *Sov. Phys. Tech. Phys.* **36**, 620 (1991).

¹¹ A. R. Sorokin, *Tech. Phys. Lett.* **29**, 171 (2003).

¹² E. Colavita *et al.*, *Phys. Rev. B* **27**, 1653 (1983).

¹³ B. L. Henke, E. M. Gullikson, and J. C. Davis, *At. Data Nucl. Data Tables* **54**, 181 (1993).

¹⁴ V. E. Cosslett and R. N. Thomas, *Br. J. Appl. Phys.* **15**, 883 (1964).

¹⁵ V. E. Cosslett and R. N. Thomas, *Br. J. Appl. Phys.* **15**, 1283 (1964).

¹⁶ V. E. Cosslett and R. N. Thomas, *Br. J. Appl. Phys.* **16**, 779 (1965).

¹⁷ P. F. Staub, *J. Phys. D* **28**, 252 (1995).

¹⁸ P. F. Staub, *J. Phys. D* **27**, 1533 (1994).

¹⁹ M. R. Sogard, *J. Appl. Phys.* **51**, 4412 (1980).

²⁰ J. A. Cline, C. D. Jonah, and D. M. Bartels, *Rev. Sci. Instrum.* **73**, 3908 (2002).

²¹ A. Haapalinn, T. Kubarsepp, and P. Karha, *Meas. Sci. Technol.* **10**, 1075 (1999).

²² J. A. Batista *et al.*, *Anal. Sci.* **17**, 73 (2001).

²³ J. L. Schiff, *Laplace Transform: Theory and Applications* (Springer, New York, 1999).